Available online at www.sciencedirect.com
SCIENCE DIRECT®
Cement & Concrete Composites 27 (2005) 471–480
Cement & Concrete Composites
www.elsevier.com/locate/cemconcomp

# Flexural strengthening of concrete beams with CFRP laminates bonded into slits

J.A.O. Barros *, A.S. Fortes

*Department of Civil Engineering, School of Engineering, University of Minho, Azurém, 4810-058 Guimarães, Portugal*

Received 17 February 2003; accepted 14 July 2004

**Abstract**

Near surface mounted (NSM) strengthening technique using carbon fibre reinforced polymer (CFRP) laminate strips was applied for doubling the load carrying capacity of concrete beams failing in bending. This objective was attained and the deformational capacity of the strengthened beams was similar to the corresponding reference beams. The NSM technique has provided a significant increment of the load at serviceability limit state, as well as, the stiffness after concrete cracking. The maximum strain in the CFRP laminates has attained values between 62% and 91% of its ultimate strain. A numerical strategy was developed to simulate the deformational behaviour of RC beams strengthened by NSM technique. Not only the load carrying capacity of the tested beams was well predicted, but also the corresponding deflection.
© 2004 Elsevier Ltd. All rights reserved.

*Keywords:* Carbon fibre reinforced polymer; Flexural strengthening; Reinforced concrete beams

## 1. Introduction

In the last decade, conventional materials, like steel and concrete are being replaced by fibre reinforced polymer (FRP) materials for the strengthening of concrete structures. These materials are available in the form of unidirectional strips made by pultrusion, in the form of sheets or fabrics made by fibres in one or two different directions, respectively, and in the form of bars. Carbon, (C)FRP, and glass, (G)FRP, are the main fibres composing the fibrous phase of these materials, while epoxy is generally used on the matrix phase. Wet lay-up (sheets and fabrics) and prefabricated elements (laminates and bars) are the main types of FRP strengthening systems available in the market. The increasing demand of FRP for structural repair and strengthening is due to the following main advantages of these composites: low weight, easy installation, high durability and tensile strength, large deformation capacity, electromagnetic permeability and practically unlimited availability in FRP sizes, geometry and dimensions [1].

The FRP laminates and sheets are generally applied on the faces of the elements to be strengthened, designated by externally bonded reinforcing technique (EBR). The research carried out up to now has revealed that this technique cannot mobilize the full tensile strength of the FRP materials, due to their premature debonding [1,2]. To improve the efficacy of the EBR technique, some anchorage systems have been proposed [3]. Since in EBR technique the FRP materials are externally exposed, the reinforcing performance of these composites can be negatively affected by the effect of freeze/thaw cycles [4] and decreases significantly when submitted to high and low temperatures [5]. EBR systems are also susceptible to vandalism acts.

To overcome these drawbacks some attempts have been made, a promising one is the near surface mounted (NSM) strengthening technique, based on the concept of

* Corresponding author.
*E-mail address:* barros@civil.uminho.pt (J.A.O. Barros).

0958-9465/$ - see front matter © 2004 Elsevier Ltd. All rights reserved.
doi:10.1016/j.cemconcomp.2004.07.004

embedding glass or carbon FRP bars into grooves made on the concrete cover of the elements to be strengthened [6]. The bond performance of this technique has been extensively analyzed in the last years [7]. This technique was used in some practical applications [8–11] and several benefits were pointed out.

With the same purpose, Blaschko and Zilch [12], and Barros and Fortes [13] applied the NSM technique where CFRP laminate strips were bonded into slits made on the concrete cover. The obtained results have shown that this is a promising technique. Tests with concrete columns strengthened by this technique have shown that the peeling can be prevented and the tensile strain of the CFRP can attain values near its ultimate strain [14].

To assess the efficacy of this strengthening technique in beams failing in bending, four series of beams were tested under four point loads. The increase of the load at serviceability and at ultimate limit states, the beam stiffness, the maximum strain of the CFRP, and the beam deflection capacity (an indicator of ductility) provided by this strengthening technique were the main aims of the experimental program. To verify whether the proposed strengthening process could double the load capacity of the reference beams was a further aim.

Material nonlinear finite elements models can be used to simulate the behaviour of RC beams strengthened by NSM technique [13,15]. These types of model are, however, very time consuming and require expert users. A simpler numerical strategy was developed to evaluate the load–deflection response of these types of structural elements.

The present work describes the carried out tests and presents the main results. The developed numerical strategy is presented and its performance was compared with the results of the tested beams.

## 2. Beams and strengthening technique

### 2.1. Beams

Fig. 1 represents the geometry of the beams, the reinforcement arrangement and the number and position of the CFRP laminates. The loading and the support conditions are also shown. Due to the process of casting, small differences in the height of the beams have oc-

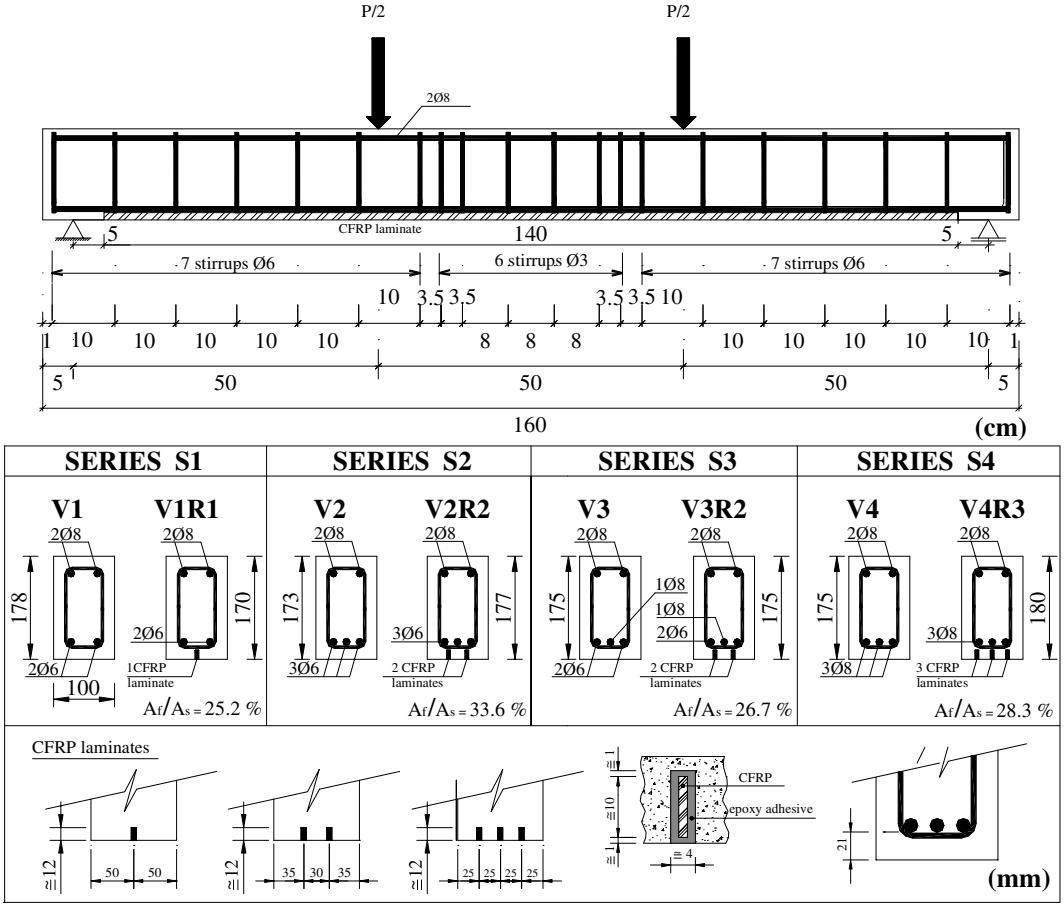


Fig. 1. Series of tested beams.

curred. The cross sectional area of the CFRP laminates ($A_f$) applied in the beam of each series (each series is composed of two beams) was evaluated for doubling the ultimate load of the corresponding reference beam. To perform this task, a cross section layer model described elsewhere [16] was used. The number of CFRP laminates was chosen to obtain the cross sectional area, as close as possible, to the value determined from the numerical analysis. The percentage of stirrups was determined to ensure bending failure modes for all beams. In Fig. 1 $A_s$ is the cross sectional area of the tensile longitudinal steel bars.

### 2.2. Strengthening technique

The strengthening technique consists of the following procedures [13]:

- slits of about 4.0 mm width and 12 mm depth were cut in the concrete cover on the tension face of the beam, using a diamond cutter (see Fig. 1);
- the slits were cleaned by compressed air;
- the CFRP laminates were cleaned by acetone;
- the epoxy adhesive was prepared according to the supplier recommendations;

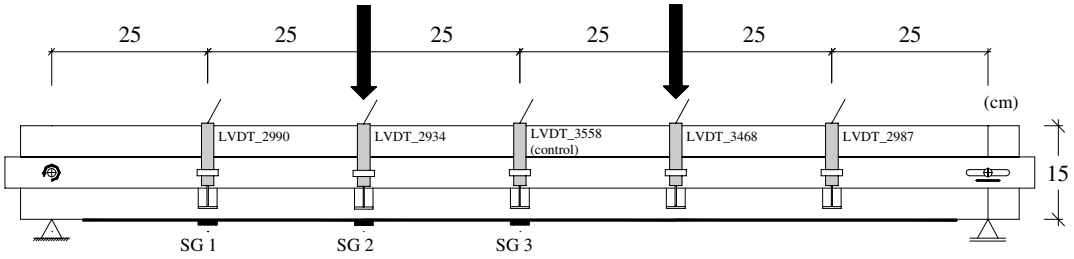


Fig. 2. Measuring devices (SG—strain gauges).

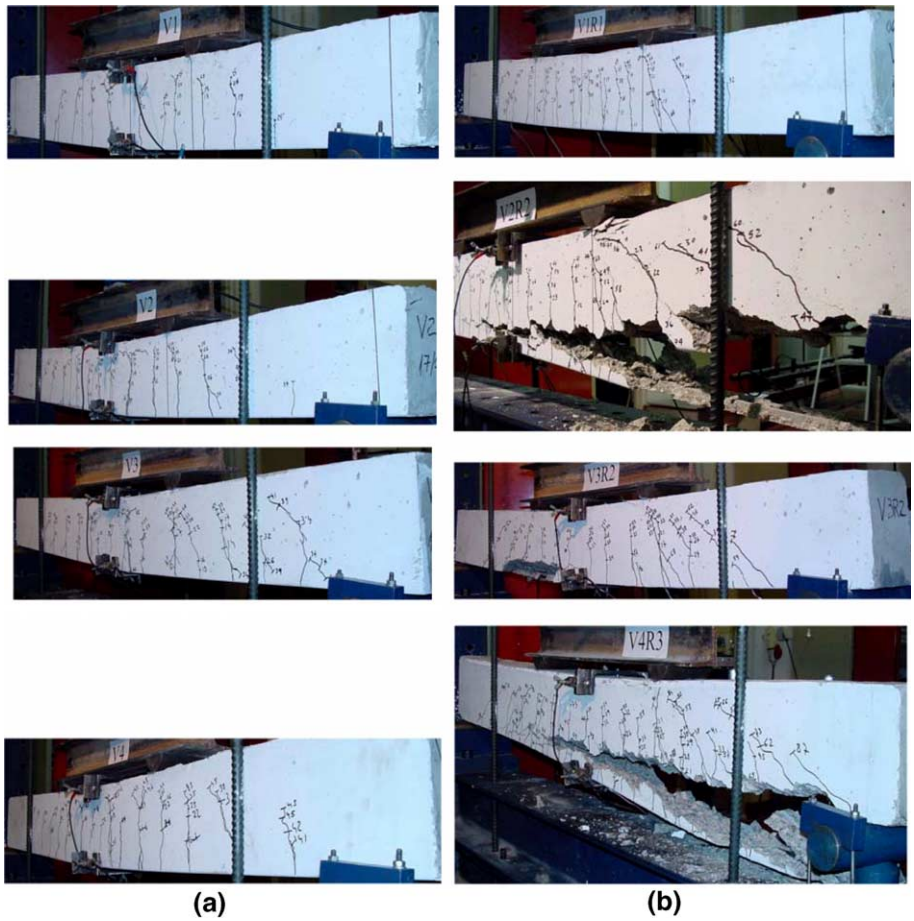


Fig. 3. Crack patterns and failure modes of (a) reference beams and (b) strengthened beams after failure.

- the slits were filled with the epoxy adhesive;
- the epoxy adhesive was applied on the faces of the CFRP laminates;
- the CFRP laminates were introduced into the slits and the excess epoxy adhesive was removed.

At least five days were spent on the curing/hardening process of the epoxy adhesive, before testing the beam.

## 3. Materials

### 3.1. Concrete

The compression strength of the concrete was determined from uniaxial compression tests carried out on cylinders of 150 mm diameter and 300 mm height, at the age of about 90 days, when the beams were tested. The concrete average compressive strength was 46.1 MPa, with a standard deviation of 2.6 MPa and a coefficient of variation of 5.7%.

### 3.2. Steel bars

The longitudinal reinforcement consisted of steel bars of 6 mm and 8 mm diameter. For shear, stirrups of 6 mm and 3 mm diameter were used. The properties of these bars are included in Table 5.

### 3.3. CFRP laminates

The CFRP laminate strips were provided in rolls, and had a cross section of $9.59 \pm 0.09$ mm width $\times$ $1.45 \pm 0.005$ mm thickness. To evaluate the correspond-

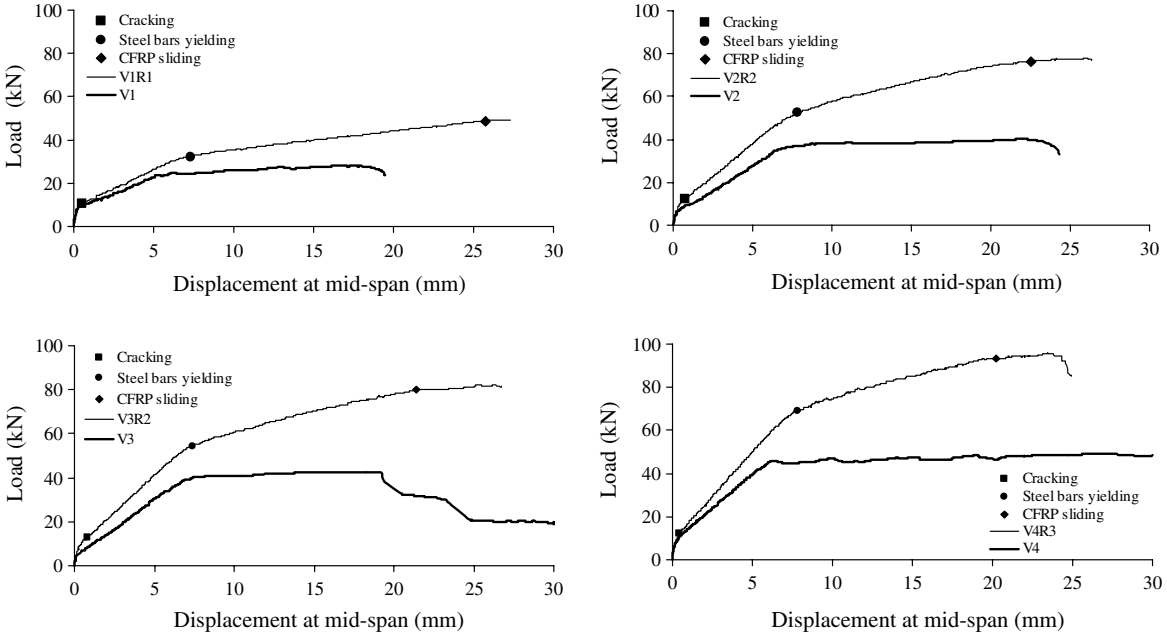


Fig. 4. Force–deflection relationships.

Table 1
Main results obtained in the series of tested beams

| Series | Beam | $P_{cr}$ (kN) | $\frac{P_{cr}\ (VR)}{P_{cr}\ (V)}$[a] | $P_{serv}$ (kN) | $\frac{P_{serv}\ (VR)}{P_{serv}\ (V)}$ | $P_{sy}$ (kN) | $\frac{P_{sy}\ (VR)}{P_{sy}\ (V)}$ | $P_u$ (kN) | $\frac{P_u\ (VR)}{P_u\ (V)}$ |
|---|---|---|---|---|---|---|---|---|---|
| S1 | V1 | 8.5 | 1.26 | 18.6 | 1.22 | 24.5 | 1.32 | 28.2 | 1.78 |
| | V1R1 | 10.7 | | 22.7 | | 32.31 | | 50.3[b] | |
| S2 | V2 | 8.1 | 1.52 | 21.7 | 1.45 | 37.5 | 1.39 | 41.0 | 1.91 |
| | V2R2 | 12.3 | | 31.4 | | 52.28 | | 78.5 | |
| S3 | V3 | 7.9 | 1.51 | 23.8 | 1.38 | 40.0 | 1.36 | 41.3 | 1.98 |
| | V3R2 | 11.9 | | 32.8 | | 54.52 | | 81.9 | |
| S4 | V4 | 8.1 | 1.74 | 32.3 | 1.25 | 46.9 | 1.47 | 48.5 | 1.96 |
| | V4R3 | 14.1 | | 40.4 | | 69.11 | | 94.9 | |

[a] VR—strengthened beam; V—reference beam.
[b] The test was interrupted when the deflection at mid span was about 27 mm.

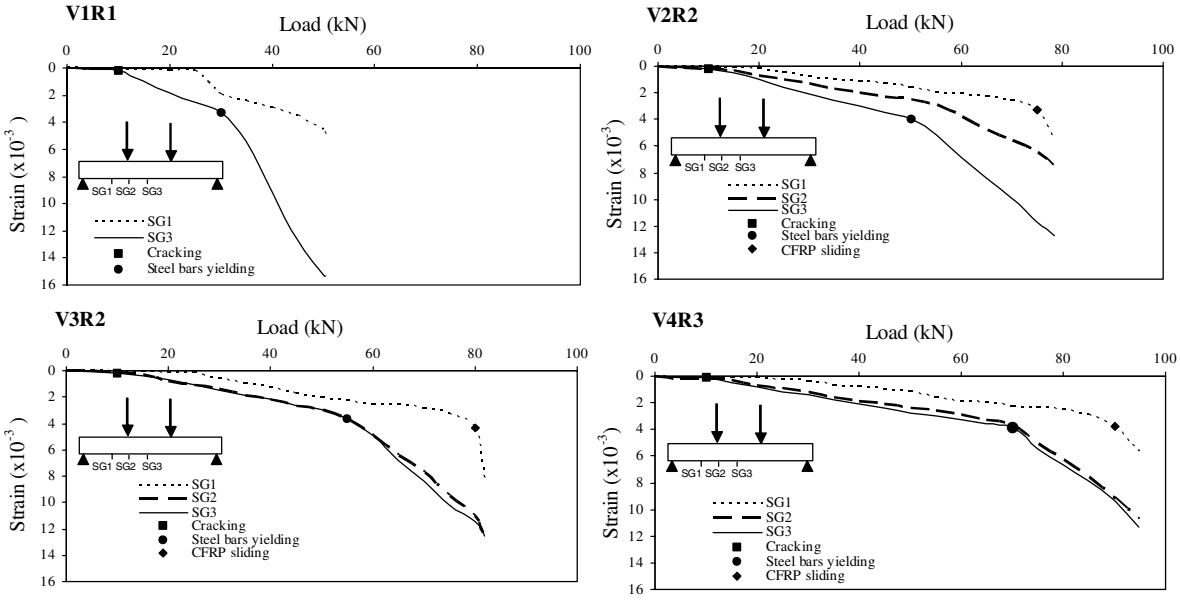


Fig. 5. Force–strain relationships.

Table 2
Maximum strains in CFRP laminates

| Series | Beam | $\varepsilon_f$ (‰) |
|---|---|---|
| S1 | V1R1 | 15.5 |
| S2 | V2R2 | 12.8 |
| S3 | V3R2 | 12.8 |
| S4 | V4R3 | 10.6 |

ing tensile strength and Young's modulus, uniaxial tensile tests were carried out in a servocontrolled test machine, according to the recommendations in ISO 5275 [17]. From these tests a Young's modulus of $158.8 \pm 2.6$ GPa, a tensile strength of $2739.5 \pm 85.7$ MPa and an ultimate strain of $17.0 \pm 0.4$‰ were obtained.

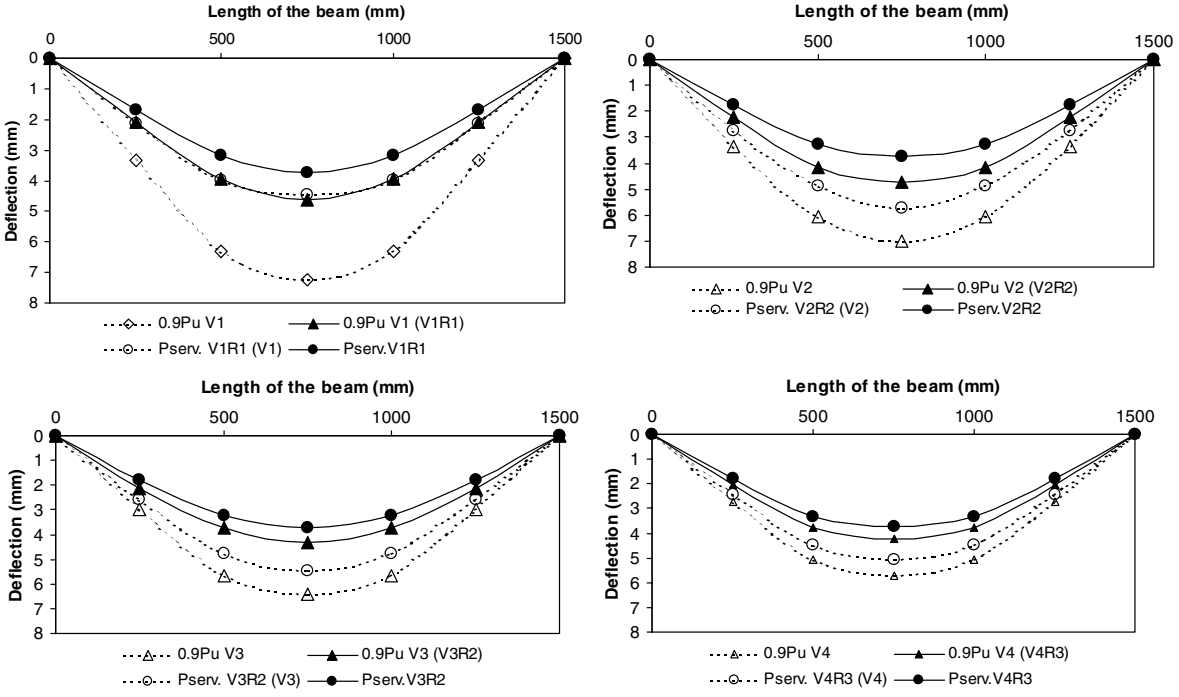


Fig. 6. Deflection of the beams.

### 3.4. Epoxy adhesive

An epoxy adhesive was used to bond the CFRP laminates to the concrete. From the uniaxial tensile tests carried out according to the recommendations in ISO 527-3 [18], a Young's modulus of 5.0 GPa and a tensile strength of 16–22 MPa were obtained [19].

## 4. Test configuration and measuring devices

LVDTs with ±12.5 mm and ±25 mm of nominal stroke and with linearity greater than ±0.1% of the full stroke were used as illustrated in Fig. 2. The LVDTs were supported on a Japanese Yok system to avoid any anomalous readings [20]. The strain gauges (SG) were mounted on the sides of the CFRP laminates and were positioned according to Fig. 2. The tests were carried out under the displacement control, imposing a displacement ratio of 20 μm/s in the LVDT at mid span. The forces were evaluated from a load cell of 200 kN capacity with ±0.05% accuracy.

## 5. Results

### 5.1. Failure modes

Fig. 3 includes the views of the beams after failure. The crack patterns on the reference beams basically consist of flexural cracks. The longitudinal steel bars in tension have yielded and the tests were interrupted when

Table 3
Increase of stiffness provided by NSM strengthening technique at two load levels

| Series | Beam | At service load of the strengthened beam | | At 90% of the maximum load of the reference beam | |
|---|---|---|---|---|---|
| | | Deflection ($u$, mm) | $\frac{u_{P^V_{serv}} - u_{P^{VR}_{serv}}}{u_{P^V_{serv}}}$ (%) | Deflection ($u$, mm) | $\frac{u_{0.9P^V_u} - u_{0.9P^{VR}_u}}{u_{0.9P^V_u}}$ (%) |
| S1 | V1 | 4.55 | 1.21 (18%) | 7.25 | 1.57 (36%) |
| | V1R1 | 3.75 | | 4.62 | |
| S2 | V2 | 5.75 | 1.53 (35%) | 7.02 | 1.49 (33%) |
| | V2R2 | 3.75 | | 4.72 | |
| S3 | V3 | 5.48 | 1.46 (32%) | 6.40 | 1.47 (32%) |
| | V3R2 | 3.75 | | 4.34 | |
| S4 | V4 | 5.05 | 1.35 (26%) | 5.69 | 1.35 (26%) |
| | V4R3 | 3.75 | | 4.22 | |

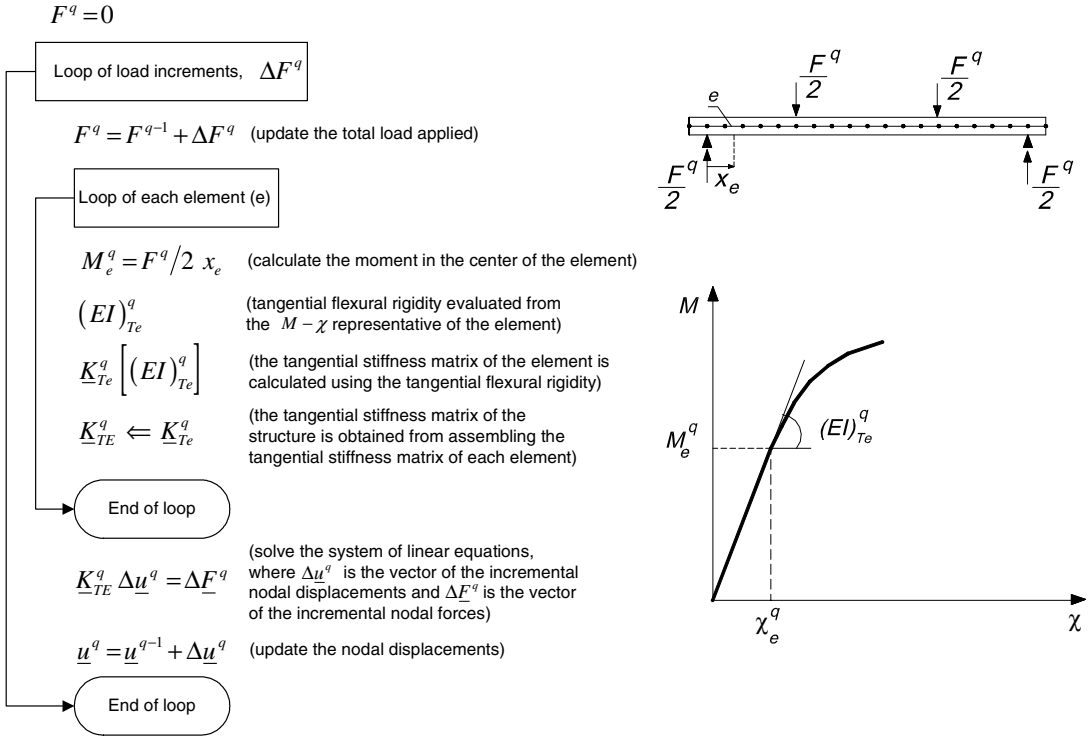


Fig. 7. Numerical approach to simulate the deformational behaviour of structural elements failing in bending.

the deflection at mid span was greater than 20 mm. Therefore, the reference beams have failed in a ductile flexural mode.

The failure mode of the strengthened beams, excepting beam V1R1, was characterized by the detachment of a layer of concrete at bottom of the beam. The detached layer was not uniform in thickness, and attained 60 mm in some parts. This reveals that, not only the concrete cover was detached, but also parts of concrete above the longitudinal reinforcement. The test of beam V1R1 was interrupted when the deflection at mid span was about 27 mm. Up to this deflection this beam had only developed flexural cracks.

### 5.2. Force–deflection relationship

The force–deflection relationship for the series of tested beams are depicted in Fig. 4, and the main results are included in Table 1. It is observed that the purpose of doubling the ultimate load ($P_u$) of the corresponding reference beam was practically attained. The increase on the load at the onset of yielding the conventional reinforcement ($P_{sy}$—yielding load) was also significant, varying from 32% to 47%. The increase on the cracking load ($P_{cr}$) was also considerable. Between the cracking load and the yielding load, the strengthened beams showed higher stiffness than their corresponding reference beams. The service load, $P_{serv}$, (the load for a deflection of $L/400 = 3.75$ mm, where $L$ is the beam span) for the strengthened beams was also increased, having been attained a maximum increase of 45%. The sliding of the CFRP laminates started to be visible before the collapse of the beam.

### 5.3. Force–strain relationship

The relationships between the applied load and the recorded strains in the CFRP laminates (see Fig. 2)

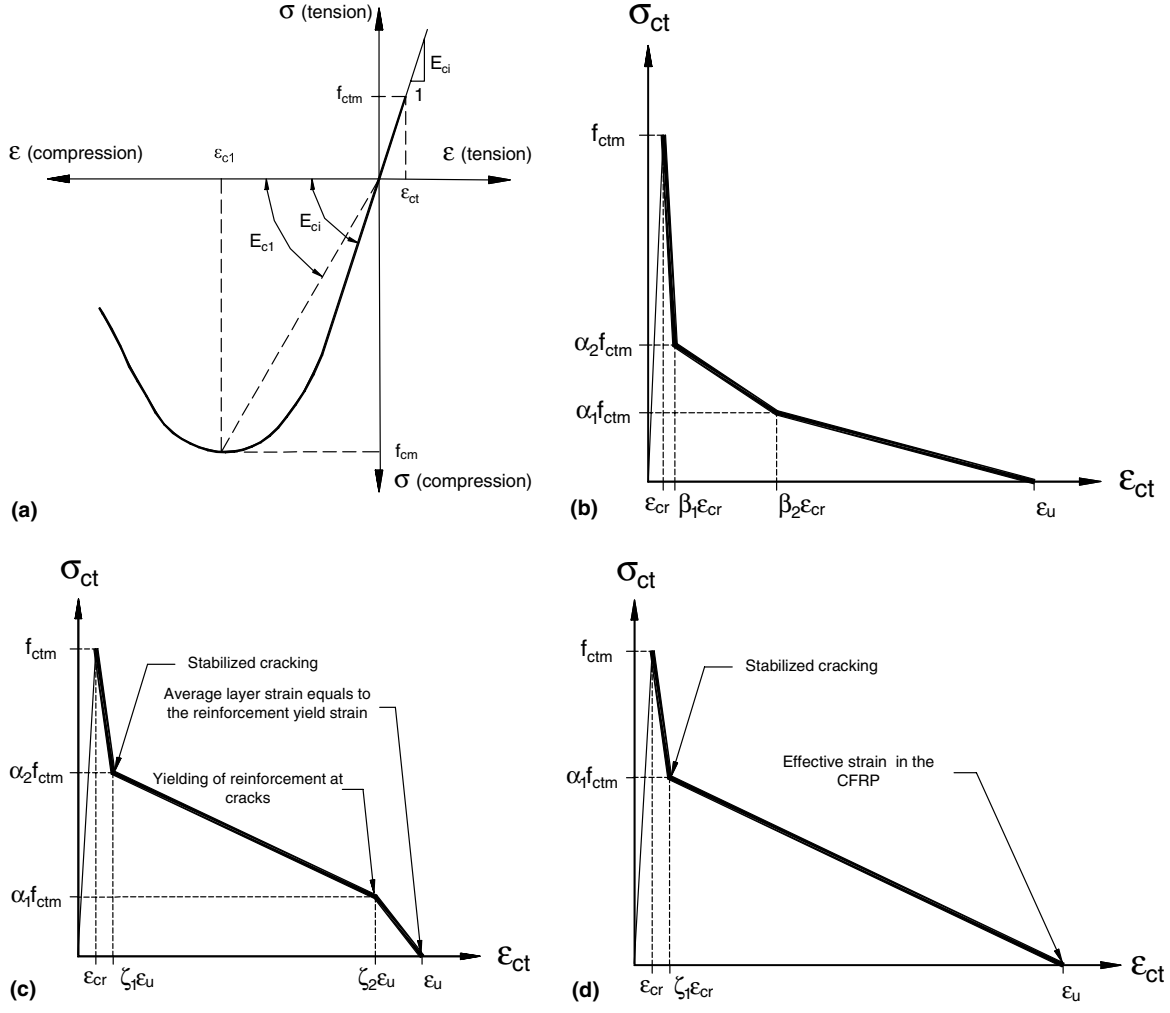


Fig. 8. Concrete laws used in the numerical simulation: (a) in compression; (b) in tension–softening; (c) in tension–stiffening of reference beams; (d) in tension–stiffening of strengthened beams.

Table 4
Concrete properties used in the numerical simulation (see Fig. 8)

| Beam | Compression | | Tension | Softening | | | | | Stiffening | | | | |
|---|---|---|---|---|---|---|---|---|---|---|---|---|---|
| | $f_{cm}$ (MPa) | $E_c$ (GPa) | $f_{ctm}$ (MPa) | $\alpha_1$ | $\alpha_2$ | $\beta_1$ | $\beta_2$ | $\varepsilon_u$ (%) | $\alpha_1$ | $\alpha_2$ | $\zeta_1$ | $\zeta_2$ | $\varepsilon_u$ (%) |
| V1 | 45.33 | 33.35 | 3.37 | | | | | 3.2 | 0.55 | 0.13 | 0.05 | 0.85 | 3.6 |
| V1R1 | | | | | | | | | 0.55 | – | 11.0 | – | 15.5 |
| V2 | 48.90 | 36.50 | 3.58 | | | | | 3.0 | 0.55 | 0.13 | 0.05 | 0.85 | 3.5 |
| V2R2 | | | | | | | | | 0.6 | – | 8.4 | – | 12.8 |
| V3 | 42.75 | 34.89 | 3.21 | 0.4 | 0.2 | 2.0 | 10.0 | 3.4 | 0.55 | 0.13 | 0.05 | 0.85 | 3.7 |
| V3R2 | | | | | | | | | 0.6 | – | 7.5 | – | 12.8 |
| V4 | 46.40 | 35.86 | 3.43 | | | | | 3.2 | 0.55 | 0.13 | 0.05 | 0.85 | 3.6 |
| V4R3 | | | | | | | | | 0.6 | – | 4.0 | – | 10.6 |

are shown in Fig. 5. The maximum strains registered in the CFRP have ranged from 62% to 91% of its ultimate strain (see Table 2).

Fig. 5 shows that the force–strain relationship is composed of three quasi-linear branches, the first one up to cracking load, the second one up to the yielding of the conventional reinforcement and the last one up to the point when CFRP begins sliding. From the first to last branch the strain ratio increases due to a decrease of the beam stiffness. In the first branch all the intervening materials behave linearly; in the second branch the concrete is cracked, the conventional reinforcement is behaving linearly and the sliding of the CFRP is marginal; in the third branch the conventional reinforcement is yielded and the sliding of the CFRP is increasing up to the development of the failure surface. As expected, in general, the strains registered in the gauges SG2 and SG3 (see Fig. 2) were similar, since they are placed in the "pure" bending region of the beam.

### 5.4. Stiffness

To estimate the increment on the beam stiffness provided by the proposed strengthening technique, the beam deflection was plotted for the two following load levels (see Fig. 6): 90% of the maximum load of the reference beam; service load of the strengthened beam. In Fig. 6, 0.9Pu V*i* and 0.9Pu V*i* (V*i*R*j*) indicate the deflection of the V*i* reference beam and the corresponding strengthened beam, respectively, at a load level of 90% of the maximum load of V*i* beam. In its turn, $P_{serv}$V*i*R*j* and $P_{serv}$V*i*R*j*(V*i*) represent the deflection of V*i*R*j* strengthened beam and the corresponding reference beam, respectively, at service load level of V*i*R*j* beam. Fig. 6 shows that the deflection of the strengthened beams was significantly lower than the deflection registered on their corresponding reference beams, revealing that the strengthening technique has increased the beam stiffness. For the serviceability limit state analysis this is an important consideration. Using the displacement at mid span for the two aforementioned load levels ($u_{P^V_{serv}}$ —reference beam; $u_{P^{VR}_{serv}}$ —strengthened beam), the increase in the beam stiffness was determined. These values are indicated in Table 3. For the service load, the average increase was 28%, while for 90% of the maximum load of the reference beam the average increase was 32%.

## 6. Numerical strategy

Previous works [20,21] have shown that, using a cross-section layered model that takes into account the constitutive laws of the intervening materials and the kinematic and the equilibrium conditions, the deformational behaviour of structural elements failing in bending can be predicted from the moment–curvature relation, $M$–$\chi$, of the representative sections of these elements, using the algorithm described in Fig. 7. To evaluate the $M$–$\chi$ relationship, the beam cross-section was discretized in layers of 1 mm thick. The beam tangential stiffness was determined evaluating the tangential stiffness matrix of the two nodes Euler–Bernoulli beam elements discretizing the beam (a mesh of 60 elements). To simulate the concrete compression behaviour, the stress–strain relationship recommended by model code CEB-FIP 1993 [22] was used (see Fig. 8a). Up to concrete tensile strength, $f_{ctm}$, the concrete was assumed behaving linearly. After peak load, the behaviour of the concrete

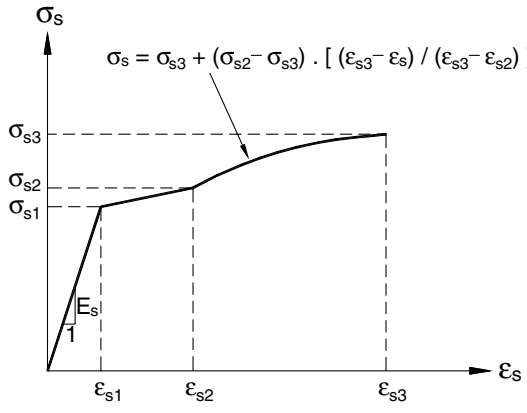


Fig. 9. Stress–strain relationship for the steel bars.

Table 5
Properties of the steel bars used in the numerical simulation (see Fig. 9)

| Bar diameter (mm) | $E_s$ (GPa) | $\varepsilon_{s1}$ (mm/mm) | $\sigma_{s1}$ (MPa) | $\varepsilon_{s2}$ (mm/mm) | $\sigma_{s2}$ (MPa) | $\varepsilon_{s3}$ (mm/mm) | $\sigma_{s3}$ (MPa) | $P$ |
|---|---|---|---|---|---|---|---|---|
| 6 | 200.0 | 0.00365 | 730.0 | 0.004 | 730.0 | 0.045 | 800.0 | 3.70 |
| 8 | 200.0 | 0.00262 | 524.2 | 0.03 | 554.2 | 0.150 | 613.5 | 2.63 |

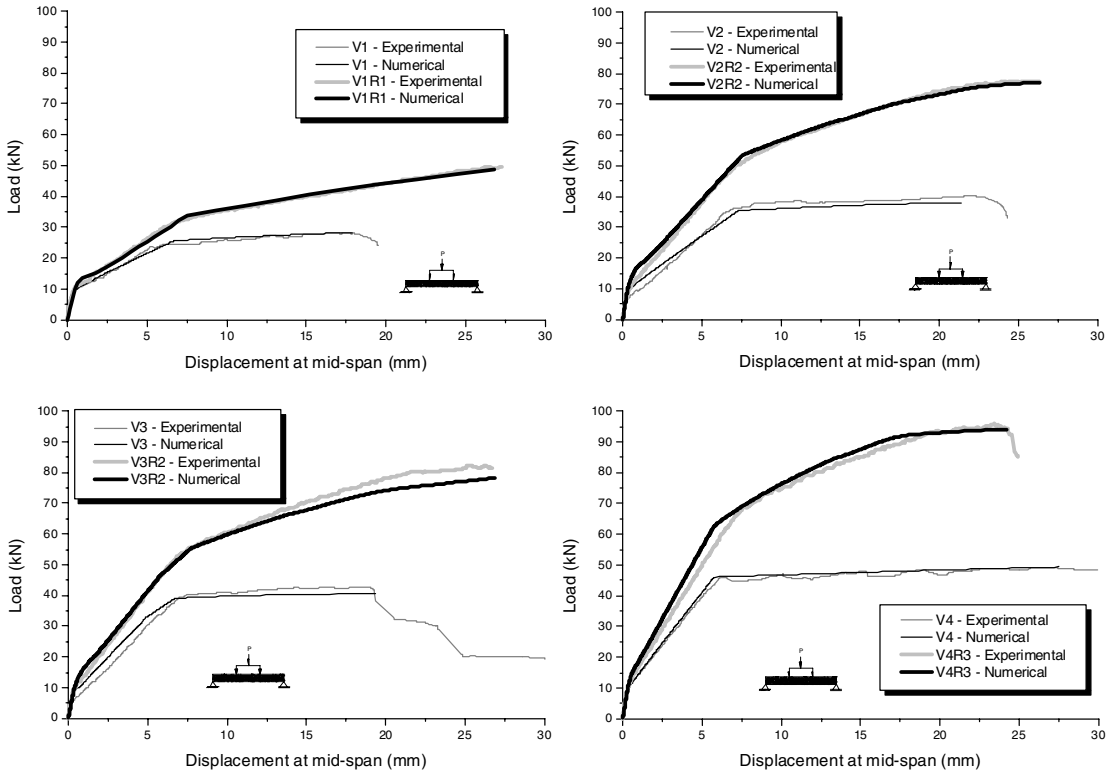


Fig. 10. Experimental versus numerical load–central deflection curves.

layers in softening [16,22] was simulated by the trilinear diagram [21] represented in Fig. 8b. The trilinear tension–stiffening diagram depicted in Fig. 8c was used to model the post-cracking behaviour of the concrete layers under the influence of the steel bars [16,22], in the case of the reference beams. For the strengthened beams, the bilinear tension–stiffening diagram represented in Fig. 8d was used, where the ultimate strain is equal to the CFRP maximum strain registered in the tested beams. The concrete data used in the numerical simulation is indicated in Table 4. Fig. 9 shows the stress–strain relationship used to model the tension and the compression behaviour of steel bars. The data defining this relationship is indicated in Table 5. A linear elastic stress–strain diagram was taken to model the tensile behaviour of the CFRP laminates.

As Fig. 10 shows, the developed numerical strategy fits with enough accuracy the registered experimental load–central deflection curves of the tested beams. This simple model can be useful to evaluate the stress and the strain levels of each intervening material during the beam loading process.

## 7. Conclusions

A strengthening technique based on applying carbon fibre reinforced polymer (CFRP) laminate strips into slits cut on the concrete cover was used with the aim of doubling the load carrying capacity of concrete beams failing in bending. This strengthening technique is designated by near surface mounted (NSM) and assured an average increase of 91% on the ultimate load of the tested RC beams. The deflection of the strengthened beams was similar to their corresponding reference beams.

Taking the results obtained it was observed that the proposed strengthening technique provided an average increase of 32% on the load corresponding to the deflection of the serviceability limit state (service load), 39% on the load corresponding to the yielding of conventional reinforcement, 28% on the stiffness for a load level corresponding to the service load of the strengthened beams, and 32% on the stiffness for a load level of 90% of the maximum load of the reference beams. The load corresponding to concrete cracking has also increased significantly. The maximum strains in the CFRP

laminates ranged from 62% to 91% of its ultimate strain, indicating that this strengthening technique can mobilize stress levels in the CFRP reinforcing elements close to the tensile strength of this composite material.

To simulate the deflection for any load level of beams failed in bending, a numerical strategy involving a cross-section layer model and the matrix stiffness method was developed. Using the properties of the intervening materials in the tested beams, obtained from experimental tests, the relationship between the force and the mid-span deflection recorded in the tested beams was predicted with high accuracy, revealing that this numerical strategy is appropriate to simulate the behaviour of RC beams strengthened by NSM technique.

## Acknowledgments

The first author wishes to acknowledge the grant SFRH/BSAB/291/2002-POCTI provided by FCT and FSE. The authors of the present work wish to acknowledge the supports provided by the S&P®, BeTTor MBT® Portugal, Secil, Solusel, and the collaboration of Cemacom. The second author acknowledges the grant provided by CAPES.

## References

[1] ACI Committee 440. Guide for the design and construction of externally bonded FRP systems for strengthening concrete structures. American Concrete Institute, ACI Committee 440, 2002, 118pp.

[2] Spadea G, Bencardino F, Swamy RN. Structural behaviour of composite RC beams with externally bonded CFRP. J Compos Constr 1998;2(3):132–7. August.

[3] Khalifa A, Alkhrdaji T, Nanni A, Lansburg S. Anchorage of surface mounted FRP reinforcement. Concrete Int: Design Constr 1999;21(10):49–54.

[4] Toutanji H, Balaguru P. Durability characteristics of concrete columns wrapped with FRP tow sheets. J Mat Civil Eng ASCE 1998;10(1):52–7.

[5] Pantuso A, Neubauer U, Rostasy FS. Effects of thermal mismatch between FRP and concrete on bond. In: Minutes of fourth ConcreteFibreCrete meeting, Lille, France, 2000.

[6] De Lorenzis L, Nanni A, La Tegola A. Flexural and shear strengthening of reinforced concrete structures with near surface mounted FRP rods. In: Humar J, Razaqpur AG, editors. Proceedings of the third international conference on advanced composite materials in bridges and structures, Ottawa, Canada, 15–18 August 2000, p. 521–8.

[7] De Lorenzis L, Nanni A. Bond between near surface mounted FRP rods and concrete in structural strengthening. ACI Struct J 2002;99(2):123–33. March–April.

[8] Warren GE. Waterfront repair and upgrade—advanced technology demonstration. Site No. 2: Pier 12. NAVSTA San Diego, Site specific report SSR-2419-SHR, Naval Facilities Engineering Service Center, Port Hueneme, CA, 1998.

[9] Alkhrdaji T, Nanni A, Chen G, Barker M. Upgrading the transportation infrastructure: solid RD decks strengthened with FRP. Concrete Int ACI 1999;21(10):37–41.

[10] Hogue T, Cornforth RC, Nanni A. Myriad convention center floor system reinforcement. Dolan CW, Rizkalla S, Nanni A, editors. In: Proceedings of the FRPRCS-4, ACI, 1999, 1145–61.

[11] Tumialan G, Tinazzi D, Myers J, Nanni A. Field evaluation of Masonry walls strengthened with FRP composites at the Malcolm Bliss Hospital. Report CIES 99-8, University of Missouri-Rolla, Rolla, MO, 1999.

[12] Blaschko M, Zilch K. Rehabilitation of concrete structures with CFRP strips glued into slits. In: Proceedings of the twelfth international conference of composite materials, ICCM 12, Paris, France, 1999.

[13] Barros JAO, Fortes AS. Concrete beams reinforced with carbon laminates bonded into slits. 5° Congreso de Mtodos Numricos en Ingeniera, Madrid, 2002.

[14] Ferreira DRSM. Pilares de Beto Armado Reforados com Laminados de Fibras de Carbono (Concrete Columns strengthened with CFRP laminates). M.Sc. thesis. Civil Engineering Department, University of Minho, 2001 (in Portuguese).

[15] Sena-Cruz JM, Barros JAO. Modeling of bond between near-surface mounted CFRP laminate strips and concrete. Computers Struct J 2004;82(17–19):1513–21.

[16] Barros JAO, Figueiras JA. Flexural behavior of steel fiber reinforced concrete: testing and modelling. J Mat Civil Eng ASCE 1999;11(4):331–9.

[17] ISO 527-5. Plastics—determination of tensile properties—Part 5: test conditions for unidirectional fibre-reinforced plastic composites. International Organization for Standardization, Geneva, Switzerland, 1997, 9pp.

[18] ISO 527-3. Plastics—Determination of tensile properties—Part 5: test conditions for unidirectional fibre-reinforced plastic composites. International Organization for Standardization, Geneva, Switzerland, 1997, 5pp.

[19] Sena-Cruz JM, Barros JAO, Faria RMCM. Assessing the embedded length of epoxy-bonded carbon laminates by pull-out bending tests. Int Conf Compos Constr 2001:217–22.

[20] Barros JAO, SenaCruz JM. Fracture energy of steel fibre reinforced concrete. J Mech Compos Mat Struct 2001;8(1):29–45.

[21] Barros JAO, Cunha VMCF, Ribeiro AF, Antunes JAB. Post-cracking behaviour of steel fibre reinforced concrete. RILEM Mat. Struct. J., in press.

[22] CEB-FIP Model Code. Comite Euro-International du Beton, Bulletin d'Information n 213/214, 1993.